

# An integrated computer-aided decision support system for die stresses and dimensional accuracy of precision forging dies

Necip Fazil Yilmaz · Omer Eyercioglu

Received: 29 January 2007 / Accepted: 14 January 2008 / Published online: 28 February 2008  
© Springer-Verlag London Limited 2008

**Abstract** Precision forging is a field in which decision support systems can be effectively and widely applied and depends on knowledge and rules derived from the past experience of forging die design engineers. Precise components are becoming quite important in attempts to reduce cost and improve reliability. There are thus many application areas in which the rules themselves become inherent to the parts or the processes. In forging die design, dimensional accuracy is one of the main goals. The load carrying capacity and life of any forged product is greatly affected by its dimensional accuracy. To predict the precise dimension of the part and determine the die dimension for precision forging, it is necessary to analyze the factors which affect dimensional accuracy. Dimensional evolution of die and product should be analyzed at each stage of forging. In this study, both radial and tangential stresses are encountered in the determination of die stresses since cylindrical workpieces were used. In order to sustain dimensional accuracy of the forging die, differences between the forging product and the die insert such as elastic die expansion and product contraction are presented.

**Keywords** Precision forging · Die stress · Decision support system

## 1 Introduction

Precision forming processes and dimensional accuracy of forged components have a special place in forging. Due to its economical benefits, precision forming is one of the most important goals for metal forming technology to achieve. The higher dimensional accuracy of forged parts has been looked at for precision manufacturing in the forging industry, together with die life. Dimensions of the forged part are likely to be different from that of the die cavity due to the elastic characteristics of the die and workpiece and thermal influences. Among these features, the elastic behaviour of the tool and work material have greater influence on the dimensional accuracy [1].

Elastic characteristics of the die and workpiece could be varied according to the shape of the part, even for the same materials. Therefore, designers should fully recognize the elastic deformation of the die and workpiece for eliminating trial-and-error. Many researchers have studied die cavity compensation experimentally or numerically in search of the better die, die life, and process design [2–10]. As for numerical studies, Takshashi and Brebbia [11] analyzed the forging die stress with the boundary element method. Sadeghi and Dean [12] studied the dimensional accuracy of precision forged axisymmetric components. Eyercioglu [13] and Dean also studied design and manufacture of precision gear forging dies. Also, several studies referred to the dimensional accuracy and some numerical studies such as FEM, upper bound elemental technique (UBET), and the slab method were proposed for elastic characteristics of the forging tool [14–18].

Gerhard and Altan [19] stated that the structural analysis of the die and the prediction of stresses and elastic deflections are useful from die life perspective. Especially in hot forging, die

N. F. Yilmaz (✉) · O. Eyercioglu  
Mechanical Engineering Department, University of Gaziantep,  
27310 Gaziantep, Turkey  
e-mail: nfyilmaz@gantep.edu.tr



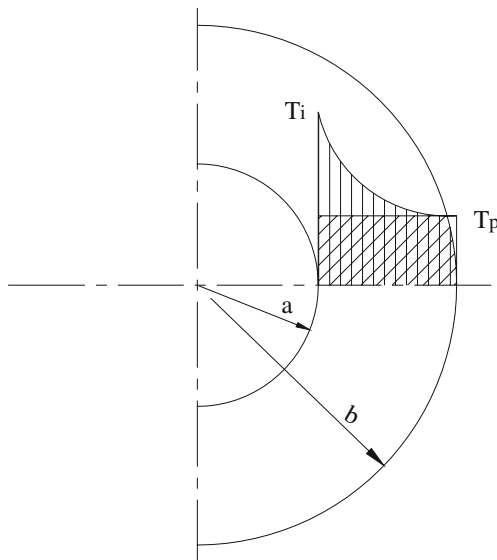


Fig. 2 Temperature distribution along the die radius in hot forging

load, the die deflection is elastic and uniform along its axis. Ignoring the friction on workpiece–die interfaces, workpiece dimensions change when the punch load is applied and removed. Also, changes in workpiece dimensions occur during ejection [25].

In order to calculate the amount of expansion of the die under radial pressure, an initially stress-free duplex cylinder is considered. By applying the punch load on the workpiece, two modes of deformation will occur. First, the workpiece will deform elastically and when the punch pressure becomes equal to the yield stress of the workpiece material, plastic deformation starts and simple compression continues until the workpiece touches the die wall. For continuity across the interface, the hoop (tangential) strains

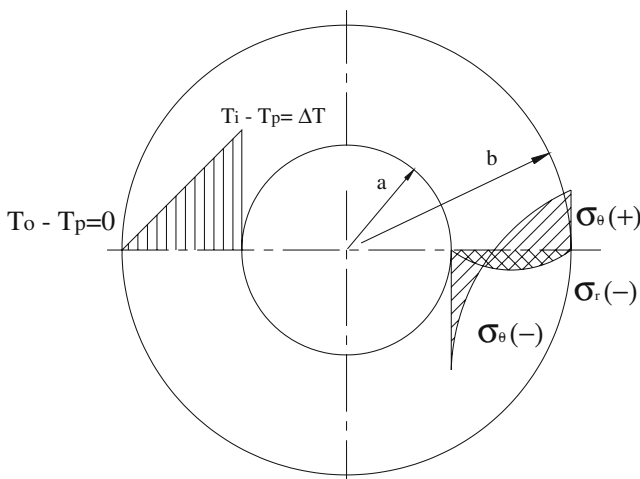


Fig. 3 Radial and tangential stress distributions due to outward temperature

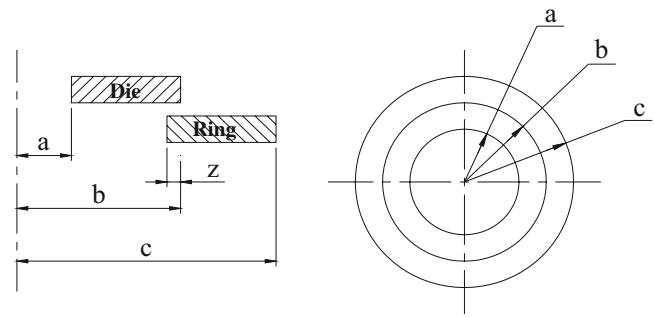


Fig. 4 Die insert and shrink ring dimensions

for insert and shrink ring must be equal at this point,  $\epsilon_{\theta 1} = \epsilon_{\theta 2}$ .

$$\epsilon_{\theta 1} = \frac{P_i \left(1 - \frac{nb^2}{a^2}\right)}{\frac{b^2}{a^2} - 1} \frac{1 - \nu_{d1}}{E_{d1}} + \frac{P_i(1 - n)}{\frac{b^2}{a^2} - 1} \frac{1 + \nu_{d1}}{E_{d1}} \quad (1)$$

$$\epsilon_{\theta 2} = \frac{nP_i}{\frac{c^2}{b^2} - 1} \frac{1 - \nu_{d2}}{E_{d2}} + \frac{nP_i \left(\frac{c^2}{b^2}\right)}{\frac{c^2}{b^2} - 1} \frac{1 + \nu_{d2}}{E_{d2}} \quad (2)$$

The subscripts 1 and 2 refer to die insert and shrink ring, respectively. When the maximum load is exerted on the workpiece, the radial stress will be greater than its yield strength. After reaching such a condition, if the punch load is removed, the die will compress the workpiece plastically until the radial stress on the workpiece is reduced to twice its shear yield stress ( $S_y$ ). By using Tresca’s yield criterion, the total amount of radial expansion of the workpiece ( $U$ ) at the end of this stage can be calculated by:

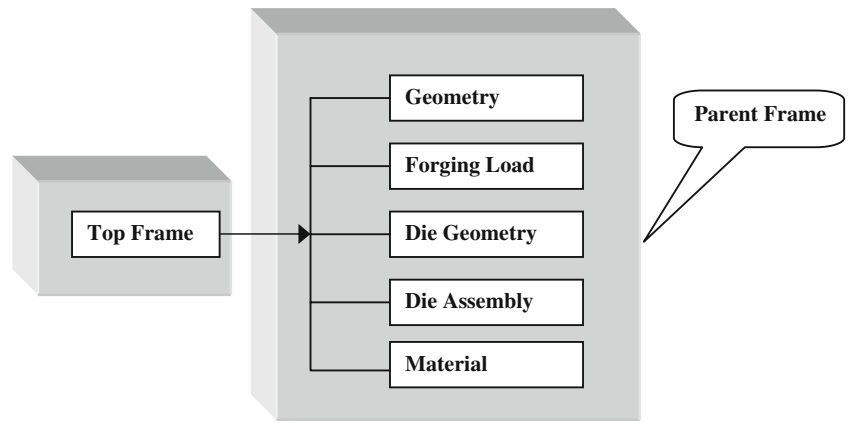
$$U_a = \frac{a(a^2(1 - \nu_{d1}) + b^2(1 + \nu_{d1} - 2n))2S_y - 2ab^2P_p}{E_{d1}(b^2 - a^2)} \quad (3)$$

At the end of the forging process, the punch pressure is zero and the radial stress ( $2S_y$ ) is still acting on the workpiece. On ejection, its radius will expand elastically and the amount of recovery ( $s$ ) can be calculated by assuming a cylindrical state of stress ( $\sigma_r = \sigma_\theta$ ) and by placing  $\sigma_z = 0$ , such that:

$$s = \frac{1 - \nu_w}{E_w} 2S_y a \quad (4)$$

where  $E_w$  and  $\nu_w$  are the Young’s modulus and Poisson’s ratio of the workpiece material, respectively. The total

Fig. 5 General frame structure



change in the workpiece dimensions due to elastic die expansion is given by:

$$U_e = \frac{a(a^2(1 - \nu_{d1}) + b^2(1 + \nu_{d1} - 2n))2S_y - 2ab^2P_p}{E_{d1}(b^2 - a^2)} + \frac{1 - \nu_w}{E_w} 2S_y a \tag{5}$$

3.2 Calculation of the thermal die expansion ( $U_t$ )

In hot forging, dies are preheated to prevent cracking of the die components and to reduce the cooling rate of the workpiece. Some heat is transferred from the workpiece during forging which further heats the die. The combination of these two sources of heat causes the die to expand.

The temperature distribution along the radius of the die with a preheat temperature of  $T_p$  and bore diameter of  $T_i$  is given in Fig. 2. The preheat temperature is assumed constant throughout the die, but the heat transferred from the workpiece produces an outward heat flow with radial

temperature gradient. Assuming uniform preheating, the die wall will expand freely. The magnitude of the radial expansion ( $U_{tp}$ ) at any radius can be determined as:

$$U_{tp} = r\alpha_d(T_p - T_r) \tag{6}$$

where  $T_r$  is room temperature,  $T_p$  is preheat temperature, and  $\alpha_d$  is the coefficient of thermal expansion of the die material.

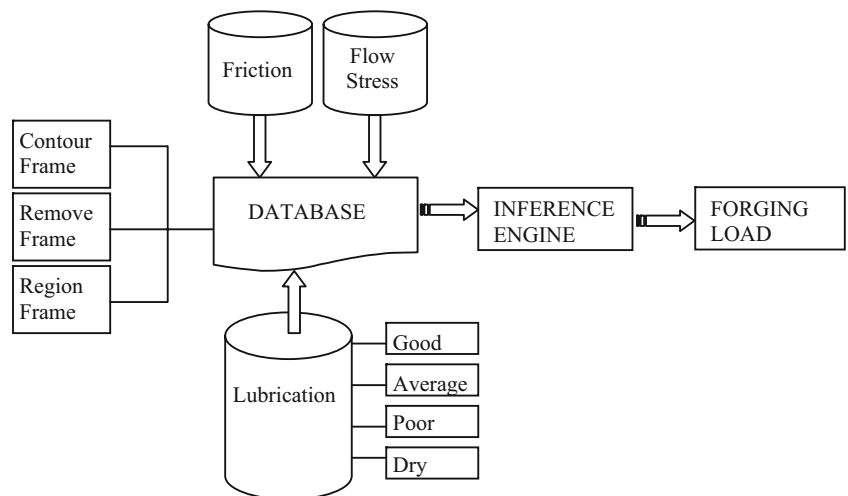
The temperature increase on the inner surface of the die and stress distributions are shown in Fig. 3. Thus, the radial displacement at any radius  $r$  due to thermal stresses can be found with:

$$U_{ts} = \frac{-\alpha_d \delta T}{3(b - a)} \left[ \frac{-(1 + \nu_d)a^2b^2}{a + b} \frac{1}{r} + (2\nu_d - 1)r^2 + \frac{(1 - \nu_d)(b^3 - a^3)}{b^2 - a^2} \right] \tag{7}$$

Total die expansion ( $U_t$ ) due to temperature will then be:

$$U_t = U_{tp} + U_{ts} \tag{8}$$

Fig. 6 Framework for forging load frame



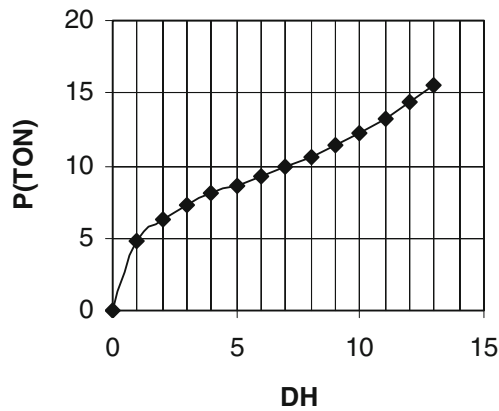


Fig. 7 Disc forging for aluminium

3.3 Calculation of the thermal product contraction ( $U_c$ )

The amount of shrinkage after hot forming operations depends on the working temperature and coefficient of thermal expansion of the forged material. Assuming that shrinkage takes place radially, and the finish forging temperature is uniform, the amount of radial contraction at any radius is:

$$U_c = r\alpha_w(T_f - T_r) \tag{9}$$

where  $T_f$  is the forging temperature,  $\alpha_w$  is the coefficient of thermal expansion of the workpiece, and  $r$  is the radius of the workpiece before contraction. In order to achieve close dimensional tolerances on forgings, die dimensions should be closely controlled. From the foregoing it is apparent that knowledge of the magnitude of the above factors should be obtained before appropriate die and electrode dimensions are determined.

Using the above analysis, the parameters affecting forging dimensions were calculated and for a given condition the profile of the die was determined. A program has been written to perform these calculations and to create the corrected forging product dimension for die. Die insert and shrink ring dimensions (Fig. 4) are then given in Eqs. 10–17.

$$b = \frac{a}{Q_1} \tag{10}$$

$$c = \frac{a}{Q} \tag{11}$$

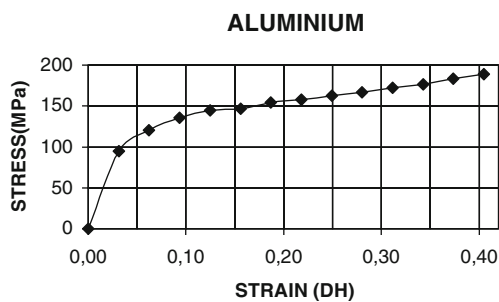


Fig. 8 Stress–strain curve for aluminium

Table 1 Aluminum ring test data

	Lubricated	Dry (ground)	Dry (rough)
$D_{o1}$ (mm)	30	30	30
$D_{o2}$ (mm)	37.7	38.5	38
$D_{i1}$ (mm)	15.2	15.2	15.2
$D_{i2}$ (mm)	14.8	13.5	11.2
$H1$ (mm)	10	10	10
$H2$ (mm)	5.65	5.35	5.3
% $\Delta H$	43.5	46.5	47
% $\Delta D$	2.63	11.18	26.3
Load (ton)	25	30	35
$m$	0.25	0.4	0.6

$$z = \frac{b \cdot S_y}{E} \left( \frac{1}{K_1} - Q_1^2 \right) \tag{12}$$

$$Q = Q_1 \cdot Q_2 \tag{13}$$

$$Q_1 = \sqrt{\frac{1}{2} \left( 1 + \frac{1}{K_1} \right) - PP} \tag{14}$$

$$Q_2 = Q_1 \cdot \sqrt{K_1} \tag{15}$$

$$PP = \frac{P_i}{S_{ydie}} \tag{16}$$

$$K_1 = \frac{S_{ydie}}{S_{yring}} \tag{17}$$

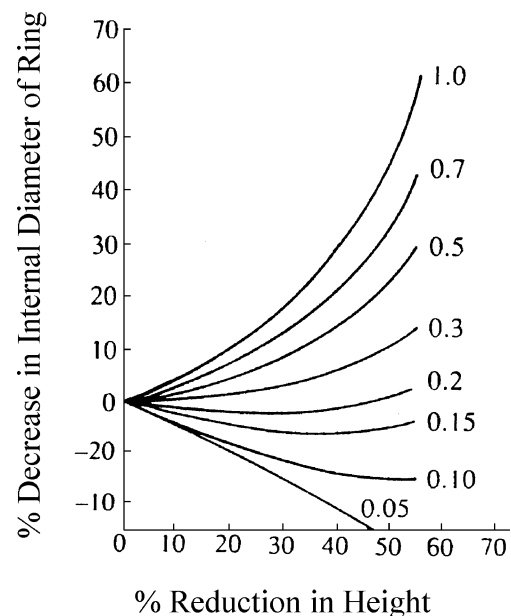


Fig. 9 Friction calibration curve in terms of  $m$  [27]

where  $a$  is the die insert inner radius,  $b$  is the die insert outer radius,  $c$  is the shrink ring outer radius,  $z$  is the interference, and  $P_i$  is the inner pressure.

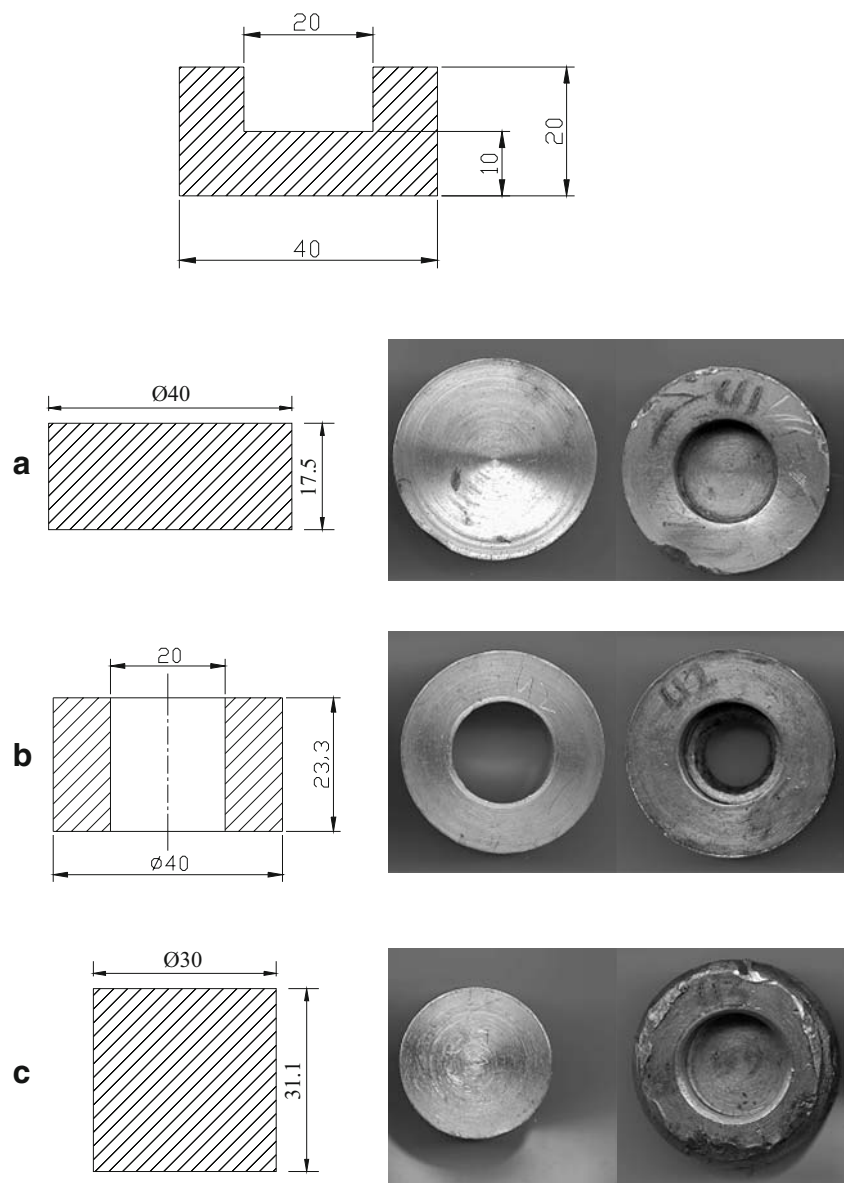
#### 4 General structure of the system

A general structure for building up an inference and control engine for the decision-support expert system as well as an algorithm for finding a compromise solution for the die stress and dimensional accuracy of the product is achieved. By using an intelligent, knowledge-based object-oriented system, high precision manufacture of product has been put

into perspective. Knowledge representation in this work was structured in the network representation. Parent frames (geometry, forging load, die geometry, die assembly, material) are connected to the top frame. Each parent frame also has child frames. General frame structure is shown in Fig. 5.

Parent frames are used to describe the general class of objects. In a database, the data definition of a record specifies how the data is stored so that the database can search and sort through the data. To actually enter the values into the system, child frames and instances are formed to represent the specific objects. Prediction of forging load has vital importance for the dimensional

**Fig. 10** U-shaped product with different sizes of specimen



accuracy and die life. This frame has six child frames and it is defined as one of the main frames of the developed system (Fig. 6).

*Contour frame* This is the child frame of forging load parent frame. This frame takes its knowledge from the geometry parent frame. In order to determine the forging load, the contour frame is the first frame that is to be fired. The entities are searched to find the inclined lines and arcs. During this process, related rules are fired so that the entities found are inclined line or arc.

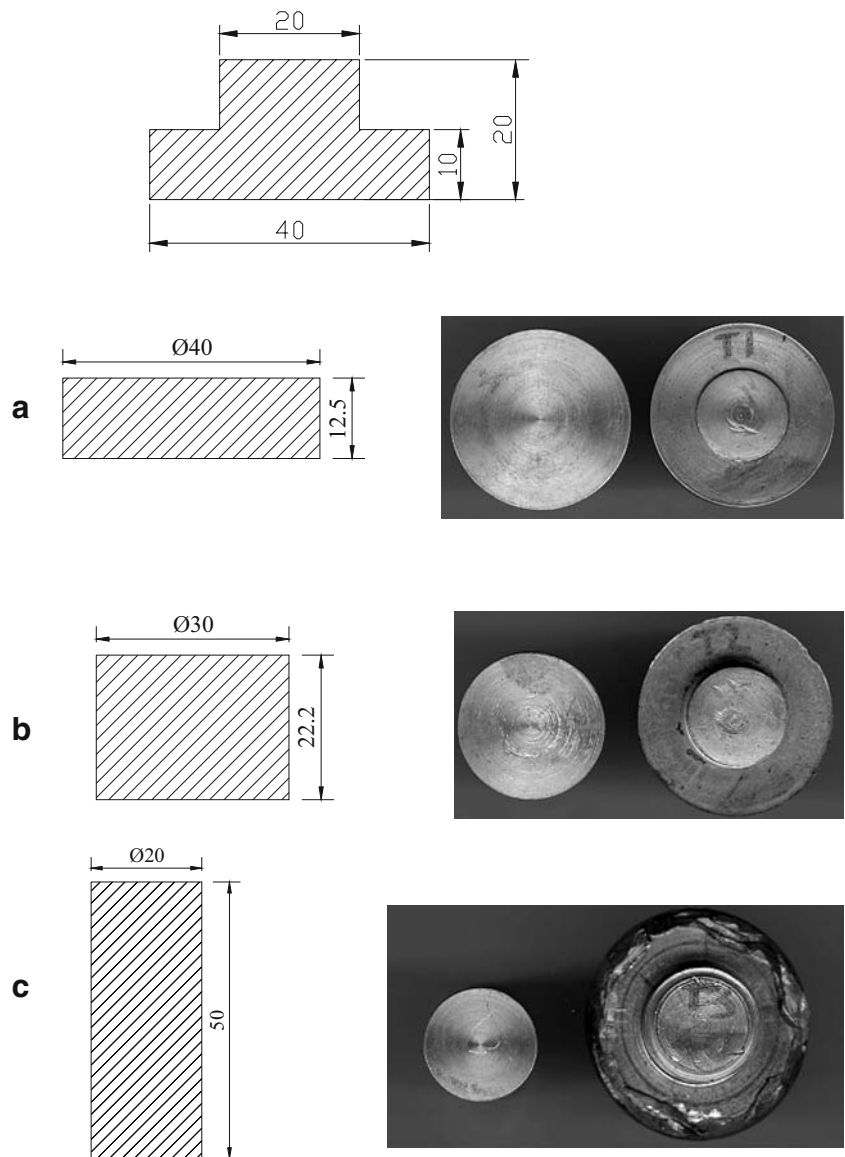
*Remove frame* This is the child frame of forging load parent frame. In this frame, removed entities are stored in the database. There are two instances. One of them contains

the knowledge about inclined lines and the other contains arcs.

*Region frame* This frame is the child frame of forging load parent frame. The geometry decomposition is made by the knowledge taken from this frame. Vertical and horizontal lines are drawn from the corners to the corresponding line. In this way, rectangular regions are obtained. The knowledge about the regions are stored in the database.

*Friction frame* One side of the region contacts one of the material, die, or punch. Therefore, each side must be checked and friction factor must be determined. This frame is used for the determination of sides, whether it contacts the material, die, or punch.

**Fig. 11** T-shaped product with different sizes of specimen



**Lubrication frame** This frame takes its knowledge from friction frame and adds its own knowledge. This frame has four slots: good lubrication, average lubrication, poor lubrication, and no lubrication (dry). These slots are required from the user. The entered values are used for the determination of friction factor for each side of the region and therefore for all forging products.

**Flow stress frame** Deformation characteristics of each material are different from the other materials. The flow stress value changes for all deformation conditions. Therefore, this property of the material must be in hand.

## 5 Experimentation

In the experiments a hydraulic press which has a capacity of 600 kN was used. A graphite–water based lubricant was

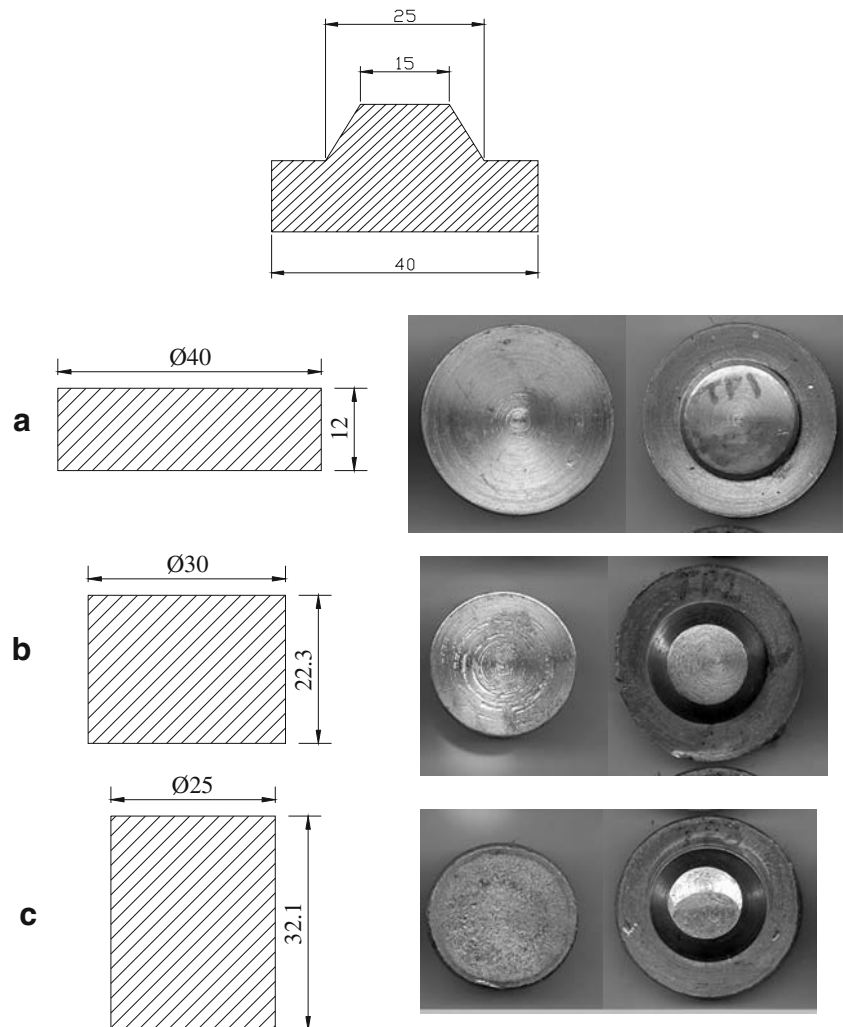
used as a lubricant. Great care was taken to ensure that all the working surfaces were completely and evenly lubricated. As a die insert material, AISI A10 air hardening medium alloy cold worked tool steel was used. The tool set comprised essentially a container, punch, ejector, and bolster.

U-shaped, T-shaped, and taper shaped aluminium products were forged. Experiments were carried out at room temperature. Three different sizes of cylindrical aluminium billets were used. Products which have a dimension of 40 mm in outside diameter and 20 mm in height were obtained from stock bars and hollow bars.

### 5.1 Disc forging

A disc forging compression test was carried out to determine the stress-strain curve for aluminium. To this aim, incremental compression was performed and after each loading, reduction of area and corresponding load were calculated and recorded.

**Fig. 12** Taper shaped product with different sizes of specimen



A reduction in height versus load graphic is shown in Fig. 7, and a stress–strain curve is shown in Fig. 8.

In order to determine the friction factor ( $m$ ), the ring compression test has been carried out. A flat ring specimen is plastically compressed between two platens. Increasing friction results in an inward flow of the material and decreasing friction results in an outward flow of the

material. For a given percentage of high reduction during compression test, the corresponding measurement of the internal diameter of the test specimen provides a quantitative knowledge of the magnitude of the prevailing friction coefficient at the die and workpiece interface [26, 27].

From this perspective, ring compression test data for aluminum are presented in Table 1.  $\% \Delta H$  and  $\% \Delta D$  values

**Fig. 13** **a** Die stress calculation screen. **b** Corrected die dimensions

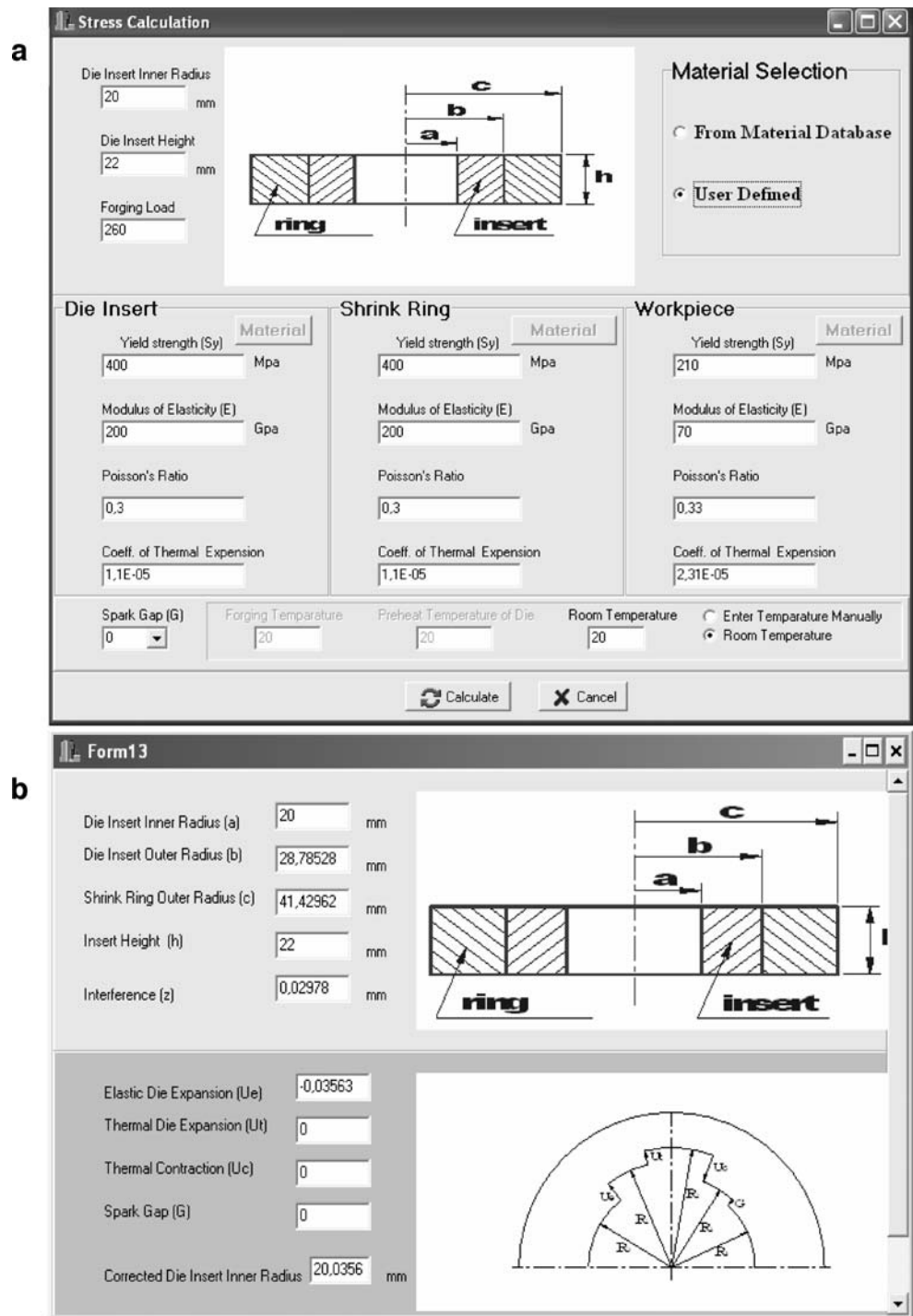


**Fig. 14** Print screen of Excel sheet

	A	B	C	D	E	F	G	H	I	J
1		Die Insert		Shrink Ring		Workpiece				
2	a (mm)	Sy (Mpa)	E (Mpa)	Sy (Mpa)	E (Mpa)	Sy (Mpa)	E (Mpa)	F (N)		
3	20	400	200000	400	200000	250	70000	260000		
4										
5	INPUT									
6	poisson Die	poisson Ring	poisson W	alfa (die)	alfa (ring)	alfa (workp)	Tp (preheat)	Tr (room)	Tf (forging)	Spark Gap
7	0,3	0,3	0,33	1,10E-05	1,10E-05	2,31E-05	25	25	25	0
8										
9										
10	Area (mm2)	Inner Pi	Pp	K1	O1	O2	O	b (mm)	c (mm)	z (mm)
11	1256,63706	206,901426	0,517253565	1	0,6947996	0,694799565	0,482746435	28,78528	41,42961719	0,02977858
12										
13		ALERT for insert material					No problem			
14		ALERT for Pp					NO PROBLEM			
15										
16	x	y	z	w	n					
17	-1,4	0	0	2	1,4285714					
18										
19										
20				Ue		-0,03563				
21				Final Wp Radius		19,96437				
22				Final Die Radius		20,03563				
23				b		28,78528				
24				c		41,42962				
25				z		0,02978				
26										

are obtained by the following equations and friction coefficient  $m$  is found from Fig. 9.

$$\% \Delta H = \frac{H_1 - H_2}{H_1} * 100$$

$$\% \Delta D = \frac{D_{i1} - D_{i2}}{D_{i1}} * 100$$

### 5.2 U-shaped forging

In precision forging of the products, complete filling of the die is regarded as the most important criterion for improving the dimensional accuracy of the forged part. The volume of the preform should be carefully controlled, otherwise underfilling or overloading of the tools may occur. It can generally be said that metal does not flow easily through the corners. Complete filling can be satisfactorily achieved by using appropriate initial billet geometry.

Figure 10 shows the dimensions of the U-shaped forging produced from three different sizes of billets by keeping their volume constant. The first one was forged from solid cylindrical bar and the product was obtained with 26 tons of load. The second one (Fig. 10b) was subjected to 55 tons of load, but the inner side of the specimen could not be filled. In the third one (Fig. 10c) both upsetting and extrusion type metal deformation exists. In this case the product is obtained with 40 tons of load.

### 5.3 T-shaped forging

T-shaped forging is shown in Fig. 11. Forging of this product was approached with three different sizes of specimens by keeping their volume constant.

Figure 11 shows the dimensions of the T-shaped forging produced from three different sizes of billets. Although 55 tons of load was applied, Fig. 11a shows that the T-shaped product could not be obtained and the die cavity could not be filled completely. But the second one was subjected to 40 tons of load and the die cavity was almost filled. The third specimen has the same diameter in the smaller part of the shape and 26 tons of load was enough to obtain this product.

### 5.4 Taper-shaped forging

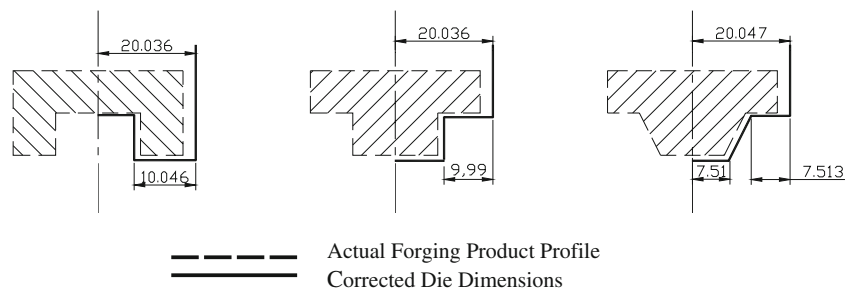
Taper shaped forging is shown in Fig. 12. This product used different sizes of specimens while keeping their volume constant. Figure 12 shows the dimensions of the taper shaped forging produced from three different sizes of billets.

Figure 12a shows that taper shaped product could not be obtained by 55 tons of load since the preform is completely subjected to the extrusion mode of deformation. But in the second trial 30 mm diameter of billet was used and the product was obtained with 35 tons of load (Fig. 12b). In this forging, the top of the taper could not be formed

**Table 2** Corrected die geometry dimensions (mm)

	U shape	T shape	Taper shape
$U_e$	-0.03563	-0.03563	-0.04667
Final workpiece radius	19.96437	19.96437	19.95333
Final die radius	20.03563	20.03563	20.04667
$b$	28.78528	28.78528	27.66765
$c$	41.42962	41.42962	38.27494
$z$	0.02978	0.02978	0.02642
$w_1$	9.98815	10.0456	7.51274
$w_2$	10.0456	9.98815	7.5110

**Fig. 15** U-, T-, and taper-shaped die cavities and the resulting product profiles



completely. The third specimen, having a diameter of 25 mm, was subjected to 24 tons of load and the required product was obtained in almost its desired dimensions.

These experiments show that the product can be obtained in different forging loads depending on the initial billet geometry due to the fin formation, upsetting or extrusion mode of deformation, and friction effect.

### 5.5 Dimensional accuracy analysis

Since the die for precision forging experiences very high radial pressure during the process, it considerably deforms in the radial direction. Therefore this radial deformation of the die becomes an important factor influencing the dimensional accuracy of the product. In order to obtain a product with accurate dimension, it is essential to evaluate the elastic deformation ( $U_e$ ) of the die and the product.

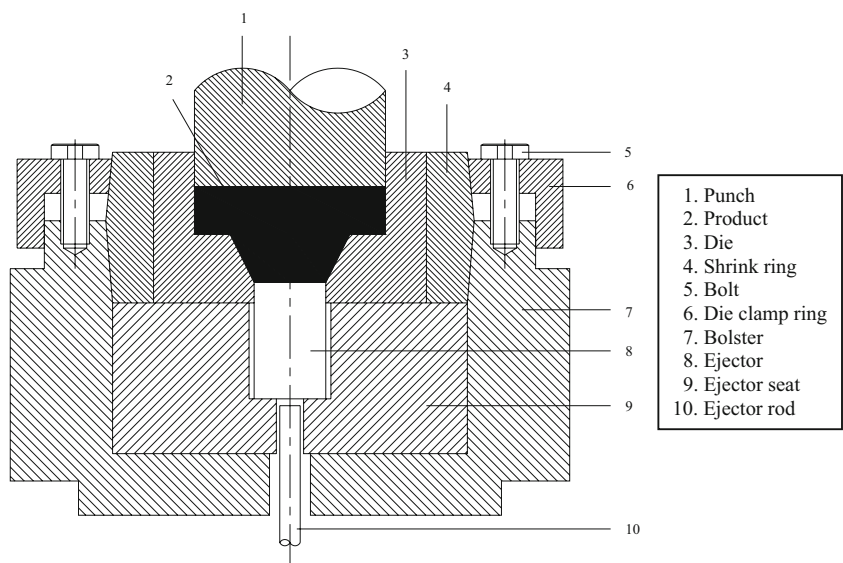
Using the above analysis, the parameters affecting forging dimensions, i.e. elastic die expansion ( $U_e$ ), were calculated by using Eq. 5 and for a given condition the dimension of the die was determined. The stress calculation screen and the corrected die dimensions for U-shaped forging, as an example, are shown in Figs. 13a and b, respectively.

The results and calculations obtained were also verified in the Excel sheet shown in Fig. 14.

According to the die stress and dimensional accuracy calculations, U-shaped, T-shaped, and taper-shaped die cavities are tabulated in Table 2 and the resulting forged profiles are given in Fig. 15.

The die design considerations for taper-shaped products are shown in Fig. 16. The punch is shown as a single unit and detail of the punch is not given. The punch forms the top surface of a cavity and is attached to the moving ram of a forging machine. The ejector is used to remove the product from the die without imposing deformation. The ejector is also used to give the shape to the bottom side of the product. The die insert forms the inner side of the die (die cavity). Since the die insert is subjected to forging load, friction load, and temperature, its material must be chosen so that it is robust in all required conditions. In order to increase the resistance against internal pressure, it is usual to make an insert shrink fitted into one or more shrink rings. The compressive stress imposed by the shrink ring has a cumulative effect at the bore of the die insert. Therefore, resultant tensile stress on the bore, caused by the forging loads transmitted through the forging part, can be substantially reduced.

**Fig. 16** General assembly of die shape



## 6 Conclusion

Computer-aided determination of forging design holds great importance for preserving the gradually disappearing know-how for the forging industry. The developed decision support system has wide applicability since the forging shapes, which are partly presented in this work, represent a large proportion of the total industrial parts. It is assumed that in axisymmetric closed die forgings, after removing the applied load, all dimensional changes take place in the radial direction. In order to study the basic mechanics of dimensional variations in a precision forging process, the case of a solid cylinder forged at room temperature in a cylindrical die is considered. A theoretical and experimental analysis of the dimensional accuracy of such a forging is presented by determining the above factors. U-, T- and taper-shaped products were forged. Although work hardening and temperature changes during forging operations were neglected, there is a close agreement between theoretical and experimental results.

**Acknowledgements** The work reported in this paper was supported by the University of Gaziantep Scientific Research Project Unit.

## References

- Lee YS, Lee JH, Kwon YN, Ishikawa T (2004) Analysis of the elastic characteristics at die and workpiece to improve the dimensional accuracy for cold forged part. *J Mater Process Tech* 153–154:1081–1088
- Peng X, Quin Y, Balendra R (2003) FE analysis of springback and secondary yielding effect during forward extrusion. *J Mater Process Tech* 135:211–218
- Park YB, Lee KH (2001) Study on the deformation of die and product in closed die upsetting. *J Mater Process Tech* 118:417–421
- Lee Y, Lee J, Ishikawa T (2002) Analysis of the elastic characteristics at forging die for the closed forged dimensional accuracy. *J Mater Process Tech* 130:532–539
- Fujikawa S, Ishihara A (1997) Development of expert systems for forging processes. *J Soc Automot Eng Japan* 18:127–133
- Park YB, Lee KH (2001) Study on the deformation die and product in closed die upsetting. *J Mater Process Tech* 118:417–421
- Koç M, Arslan M (2003) Design and finite element analysis of innovative tooling elements (stress pins) to prolong die life and improve dimensional tolerances in precision forming processes. *J Mater Process Tech* 142(3):773–785
- Kojima Y et al (1985) Measurement of pressure distribution in drawing of bars. *J JSPE* 855–861
- Matsubara S, Kudo H (1991) Devising and calibration of a simple sensor for determining pressure distribution on tool workpiece interfaces. *J JSTP* 589–596
- Matsubara S, Kudo H (1991) Nonuniform pressure distribution on punch nose surface in axisymmetric cold forging processes. *J JSTP* 874–879
- Takshashi S, Brebbia CA (1990) Forging die stress analysis using boundary element method. *Advanced Tech Plast* 203–210
- Sadeghi MH, Dean TA (1991) Analysis of dimensional accuracy of precision forged axisymmetric components. *J Eng Manuf* 205(4):171–178
- Eyercioglu O, Dean TA (1997) Design and manufacture of precision gear forging dies. CIRP international conference on design and production of dies and molds, Istanbul, Turkey
- Yilmaz NF, Eyercioglu O (2003) Application of UBET in the prediction of forging load for axisymmetric forging. *Int J Adv Manuf Syst* 6:1–11
- Kuzman K (2001) Problems of accuracy control in cold forming. *J Mater Process Tech* 113:10–15
- Qin Y, Balendra R (1997) FE simulation of the influence of die elasticity on component dimensions in forward extrusion. *J Mach Tools Manuf* 37:183–192
- Hou J (1997) A plane strain UBET analysis of material flow in a filled deep die cavity in closed die forging. *J Mater Process Tech* 70:103–110
- Rantunga V, Gunesakara J, Frazier W, Hur K (2001) Use of UBET for design of flash gap in closed die forging. *J Mater Process Tech* 111:107–112
- Gerhard H, Atlan T (1989) Investigation of die stresses and die deflections in forging axisymmetric parts. *Steel Research N* 60:255–262
- Park YB (2001) Study on the deformation of die and product in closed die upsetting. *J Mater Process Tech* 118:417–421
- Mazyad M (2004) Computer modeling of complex metal forming processes using the upper bound elemental technique (UBET) and modified upper bound elemental technique (MUBET). PhD Thesis, Ohio University, USA
- Yilmaz NF (2002) An expert system for near net shape axisymmetric forging die design. PhD Thesis, University of Gaziantep, Turkey
- American Society for Metals (1975) Source book on cold forming. ICFG data sheet no 70003. ASM, Metals Park, Ohio
- American Society for Metals (1975) Source book on cold forming. ICFG data sheet no 6/72. ASM, Metals Park, Ohio
- Sadeghi MH (1989) Precision forging axisymmetric shapes, straight and helical spur gears. PhD Thesis, University of Birmingham, UK
- Male AT, DePierre V, Saul G (1972) The validity of mathematical solutions for determining friction from the ring compression test. *J Lubr Technol* 96:389–397
- Mielnik EM (1991) Metalworking science and engineering. McGraw-Hill, New York